



HAL
open science

Characterization of hydrogenated dentin components by advanced ^1H solid-state NMR experiments

Yannick Coppel, Yann Prigent, Geneviève Grégoire

► To cite this version:

Yannick Coppel, Yann Prigent, Geneviève Grégoire. Characterization of hydrogenated dentin components by advanced ^1H solid-state NMR experiments. *Acta Biomaterialia*, 2021, 120, pp.156-166. 10.1016/j.actbio.2020.08.022 . hal-03202730

HAL Id: hal-03202730

<https://hal.science/hal-03202730v1>

Submitted on 3 Feb 2023

HAL is a multi-disciplinary open access archive for the deposit and dissemination of scientific research documents, whether they are published or not. The documents may come from teaching and research institutions in France or abroad, or from public or private research centers.

L'archive ouverte pluridisciplinaire **HAL**, est destinée au dépôt et à la diffusion de documents scientifiques de niveau recherche, publiés ou non, émanant des établissements d'enseignement et de recherche français ou étrangers, des laboratoires publics ou privés.



Distributed under a Creative Commons Attribution - NonCommercial 4.0 International License

Characterization of hydrogenated dentin components by advanced ^1H solid-state NMR experiments

Yannick Coppel ^{a,*}, Yann Prigent ^b, Geneviève Grégoire ^c

^a *Laboratoire de Chimie de Coordination UPR8241, CNRS, 205 Rte de Narbonne, F-31077
Toulouse Cedex 04, France.*

^b *Institut de Chimie de Toulouse (ICT) - FR 2599, Faculté des Sciences et de l'Ingénierie, Université Toulouse III,
31062 Toulouse, France.*

^c *Faculté d'Odontologie, Toulouse Cedex 31062; Unité de Recherche Biomateriaux Innovants et Interfaces
EA4462/URB2i, Université Paris, 92120*

Abstract

Collecting information about molecular organisation on biological materials such as bone and dentine represents a major challenge in attaining a better understanding of their mechanical properties. To that end, solid state Nuclear Magnetic Resonance (ssNMR) spectroscopy is an appropriate strategy to provide atomic structural details on these amorphous composite materials. However, species like water molecules and hydroxyl groups are usually observed through ^1H magic angle spinning (MAS) ssNMR that suffers from poor resolution due to strong signal overlapping, making their identification difficult.

This paper proposes a set of ssNMR experiments for ^1H characterization of the main components of human dentin, based on homo- and hetero-nuclear dipolar couplings and composed mostly of fast 1D experiments. The ^1H assignment is assisted by straightforward sample modifications: vacuum drying, deuterium exchange and demineralization. These experiments allow the hydrogen signal edition of dentin species like water molecules, HPO_4^{2-} and OH^- groups, depending on their localization (bound to the organic phase, linked to apatite or at the interface) and their dynamic behaviour. This ssNMR toolbox has the potential to provide important structural and dynamic information on chemical and physical modifications of biomaterials.

Keywords: Dentin composition, solid state NMR, ^1H MAS NMR, water molecules, chemical organisation, apatitic biomaterial

1. Introduction

There is a strong demand for obtaining detailed molecular-level structural information on biological materials like bone and dentin. This information provides insights about the organization of their various constituents and on the dynamic behaviours within them. Such data could be essential for understanding the mechanical properties of these apatitic biomaterials.

Dentin is similar to bone and is composed of mineralized collagen proteins, growth factors which also comprises extracellular proteins, and water [1,2]. Despite many studies describing dentin

transformation at the cellular level and showing peritubular and intertubular differences in the mineralization front, after its formation, dentin is a rather stable structure. Yet, at the molecular level, the chemical organization is still a matter of reflection. Dentin contains about 70 wt % of a mineral phase with a complex formulation described as $\text{Ca}_{8.0}\text{Mg}_{0.4}(\text{PO}_4)_{4.4}(\text{HPO}_4)_{0.7}(\text{CO}_3)_{0.9}(\text{OH})_{0.4}$ (irrespective of sodium content) [3] and 20 wt % of organic matter [2,4]. The third main component of dentin is water (about 10 wt %) that also plays a significant structuring role [5].

The complex nature and structural disorder of these calcified biomaterials make their molecular structural characterization by biophysical techniques extremely challenging. To get deeper information, solid state magic angle spinning (MAS) Nuclear Magnetic Resonance (NMR) spectroscopy has been demonstrated to be a very powerful technique in this field. The NMR studies have mainly focused on bone materials [6-8] and those on dentin have been much scarcer [9-12]. In particular, the apatitic phase has been extensively studied using ^{31}P ssNMR [5,6,13-15]. From these analyses, it has been notably proven that the mineral part is made of an amorphous calcium phosphate (ACP) phase that covers a more crystalline hydroxyapatite core [16]. The amorphous part represents a disordered phase rich in phosphonate HPO_4^{2-} ions and structural water molecules. It corresponds to a structured hydrated surface layer with relatively mobile ions that is less stable than the crystalline apatitic domain [3]. Most of the ssNMR investigations on the organic part have concentrated on the collagen structure through ^{13}C signal measurements [5,6,14,17-20]. ^{13}C MAS NMR also highlighted the presence of citrate [21,22] and carboxylate ions CO_3^{2-} [17] in these biomaterials.

ssNMR analysis of water molecules is even more complicated because it must rely on the NMR of hydrogen atoms. Unfortunately, many different hydrogenated species are present in these mineralized tissues and ^1H MAS NMR is not considered as a high-resolution technique. Even with the help of ultrafast MAS and high-field NMR spectrometer, 1D ^1H MAS NMR spectrum of bone showed a poor resolution with strong signal overlap [23]. This ssNMR experiment does not allow a direct detailed characterization of the different hydrogenated species. In particular, the ^1H ssNMR signal of water molecules that are present in different environments (in the apatitic phase, inside collagen helices, at the inorganic-organic interface...) is poorly defined. Usually, most of the water signal is described as a broad resonance around 5 ppm. Fortunately, more information on the ^1H signals can be obtained through several 2D ssNMR experiments: $^1\text{H}/^{31}\text{P}$ and $^1\text{H}/^{13}\text{C}$ HETCOR (heteronuclear correlation) and $^1\text{H}/^1\text{H}$ dipolar correlations (DQMAS, NOESY) [5,6,14,24,25]. Use of 1D version of the $^1\text{H}/^{31}\text{P}$ HETCOR, the $^1\text{H}/^{31}\text{P}$ double cross polarization (DCP) experiment, has also been reported to edit ^1H close to ^{31}P nuclei [16]. In addition, it has been shown that some bone's ^1H resonances can be resolved using a dipolar filter [26]. Finally, 2D correlations between ^1H and the most abundant quadrupolar nucleus in bone, ^{43}Ca and ^{23}Na , has been performed with the D-HMQC (dipolar-heteronuclear multi quantum coherence) experiment [27,28]. These 2D experiments coupled with hydration level control and hydrogen/deuterium (H/D) exchange, are appropriate to study the structuring role of water in bone [19,25,29-32]. ssNMR characterizations of water molecules and their dynamics have significantly contributed to a better understanding of the physical properties of these composite biominerals.

Here, we propose a NMR protocol to study hydrogenated species of human dentin (Hu-dentin). It is composed of a set of 1D/2D ssNMR experiments and sample treatments that allow editing ^1H ssNMR signals of molecules according to their environment and mobility. This NMR toolbox was used to investigate Hu-dentin of whole teeth, rarely characterized by NMR, and its demineralized counterpart. It allows us to propose a detailed characterization of the main hydrogenated dentin species, in particular of water molecules.

2. Materials and methods

2.1 Sample preparation

Human molars were used for the study. They were healthy 3rd molars extracted for reasons of development pathology. No impacted teeth were included in the study. After extraction, the teeth were kept in chloramine T solution at 4°C until use.

Human dentin (Hu-dentin) was used here in powder form. Dentin powder was prepared as described previously [33]. Briefly, the crowns were removed from the roots using a slow speed saw (Isomet 2000; Buehler, Evanston, Ill.) equipped with a rotating diamond-impregnated copper disk (Buehler). The pulp was removed and the enamel carefully eliminated with a diamond burr under water irrigation. Dentin blocks were ground at low temperature in a grinder (K Janke & Kunkel Ika®, Labortechnik, Wasserburg, Germany) by adding nitrogen into the grinding chamber. The resulting dentin powder was sieved to obtain a powder with an average particle size of maximum 0.67 μm and then stored in the absence of moisture [34].

For demineralized samples, the dentine powder was etched by adding 35 % phosphoric acid for 15 sec. Following etching, the powder was rinsed for 30s with water and dried without overdrying. This protocol is required to avoid contraction and collapse of the demineralized collagen matrix by maintaining it in its hydrate state [35]. Vacuum dried samples were prepared by placing the sample in a vacuum chamber for one hour. Deuterium exchange was performed by wetting the samples with D_2O for 24 hours followed by 1 hour of vacuum drying.

2.2 Solid-state NMR

ssNMR experiments were recorded on a Bruker Avance 400 III HD spectrometer operating at a 9.4 T magnetic field. Samples were packed into 4 mm or 1.3 mm zirconia rotors. The rotors were spun at 10 or 60 kHz (ν_r) at 293K. ^1H MAS were performed with the DEPTH pulse sequence (Fig. 1a) and a recycle delay of 10 s. ^{31}P MAS and ^{31}P CPMAS (Cross-Polarization MAS) were done with recycle delays of 600 s and 5 s, respectively. The contact times were set between 0.2 to 10 ms. ^{13}C CPMAS have been performed quantitatively [36] with eleven 1.1-ms CP periods, 0.5 s ^1H recovery time and 2 s recycle delay. ^1H MAS with rotor synchronous dipolar filtering and spin echo excitation (DF-SE) [37] (Fig. 1b)

were acquired with a filtering time between 0.76 and 23 ms and a recycle delay of 10 s. $^1\text{H}/^{31}\text{P}$ double cross polarization (DCP) MAS [38] (Fig. 1c) were performed with a first CP transfer between 3 and 6 ms, a second CP transfer between 0.2 and 2 ms and a recycle delay of 3 s. $^1\text{H}/^{13}\text{C}$ DCP MAS were registered with a first and a second CP transfers of 3 and 2 ms, and a recycle delay of 3 s. $^1\text{H}/^{31}\text{P}$ HETCOR experiment was carried out with a contact time of 2 ms and with frequency switched Lee-Goldburg homonuclear decoupling during ^1H evolution (scaling factor of 0.57 determined by the procedure of Kumari *et al.* [39]). The 2D ^1H - ^1H double-quantum–single quantum (DQ-SQ) MAS experiments were recorded with 2 periods recoupling using the back-to-back (BABA) sequence (Fig. 1d) at a spinning frequency of 60 kHz. 2D ^1H - ^1H Single Quantum-Single Quantum (SQ-SQ, NOESY) were achieved with a mixing time of 18 ms (Fig. 1e). ^{23}Na MAS were registered with a recycle delay of 1 s. 1D $^1\text{H}/^{23}\text{Na}$ and $^1\text{H}/^{43}\text{Ca}$ D-HMQC [40] (Fig. 1f) were carried with $\text{SR}4^2_1$ dipolar recoupling of 0.8 and 1 ms, respectively. Chemical shifts were externally referenced to TMS for ^1H and ^{13}C , to 85% H_3PO_4 solution for ^{31}P and to solid NaCl (at 7.2 ppm) for ^{23}Na .

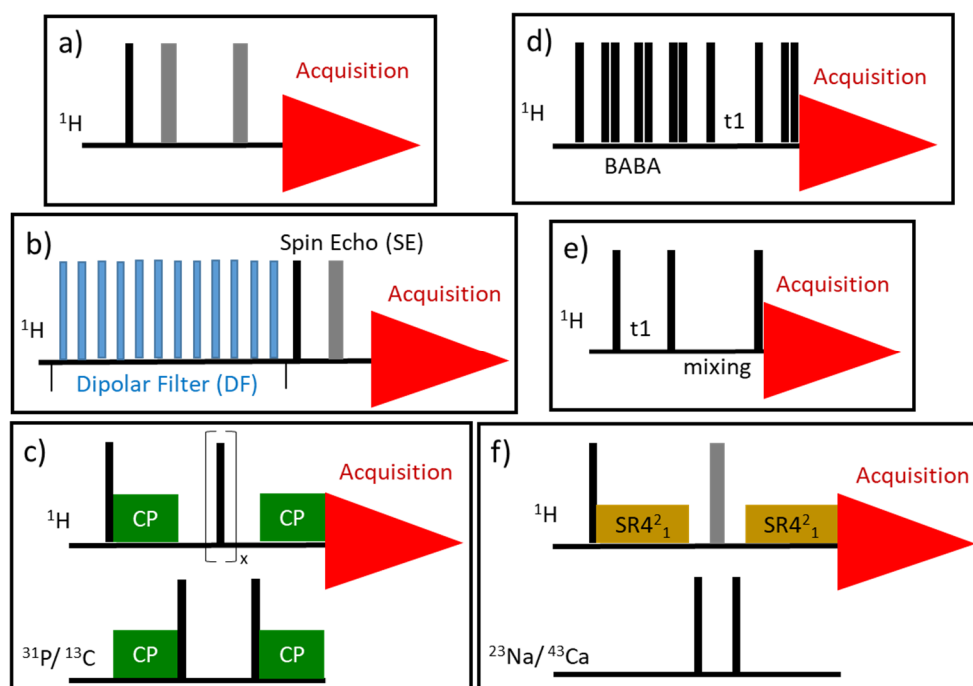


Fig. 1. NMR pulse sequences used in this work to acquire ^1H signals: a) DEPTH, b) DF-SE, c) DCP, d) DQ-SQ, e) SQ-SQ (NOESY) and f) D-HMQC.

125 3. Results and discussion

Human dentin sub-millimeter size particles were shown to conserve the representative constituents of sound human dentin including water [33]. The ^{31}P MAS spectrum of Hu-dentin (Fig. 2a) shows a single peak at ~ 3.2 ppm, characteristic of phosphate groups of carbonated apatite. This single peak is in fact an overlap of a sharp (full width at half-maximum (fwhm) height of 310 Hz) and a broad resonance (fwhm of 830 Hz) due to different phosphorus local environments. There is now a consensus in the literature that

for bone-like matrix such as dentin: the broad ^{31}P resonance is associated to an amorphous calcium phosphate (ACP) phase that covers a more crystalline apatic core (sharp ^{31}P resonance) [11,13,16,41,42]. The larger linewidth of the ACP phase is due to a distribution of ^{31}P isotropic chemical shifts associated to local disorder (inhomogeneous broadening) [43]. It has been proposed that the ACP phase contains mainly divalent species such as HPO_4^{2-} , CO_3^{2-} and Ca^{2+} and structural H_2O [31,44]. It has also been shown that the apatite core is composed of crystalline hydroxyapatite (HAp, $\text{Ca}_5(\text{PO}_4)_3\text{OH}$) and nonstoichiometric apatite (NS-HAp) [3,11]. The NS-HAp stems from incorporation of a substantial amount of anionic (mainly CO_3^{2-}) and cationic (mainly Na^+ and Mg^{2+}) substitutions, as well as to the presence of ion vacancies into the mineral structure [3,45]. ^{31}P CPMAS spectra (Fig. 2b) makes it possible to distinguish the ACP and HAp phase because their cross-polarization dynamics are strongly different. Short contact times notably enhance the ^{31}P ACP signal while long contact time favors the HAp signal [46,47].

The ^{13}C CPMAS spectrum of Hu-dentin (Fig. 2c top) is similar to published spectra of bone and dentin materials [10,18-20]. It is dominated by the signals from collagen proteins. It shows also the presence of a high concentration of citrate ions (^{13}C signal at 180.1 and 75.4 ppm) [21,22]. The ^{13}C MAS NMR spectrum also contain signals of non-collagenous macromolecules (*i.e.*, proteins, lipids, and polysaccharides) but with weak intensities due to their minor amounts. Finally, the ^{13}C signals of the carboxylate ions CO_3^{2-} were shown to overlap with those of carbonyl and carboxyl protein groups around 168 ppm [17].

150

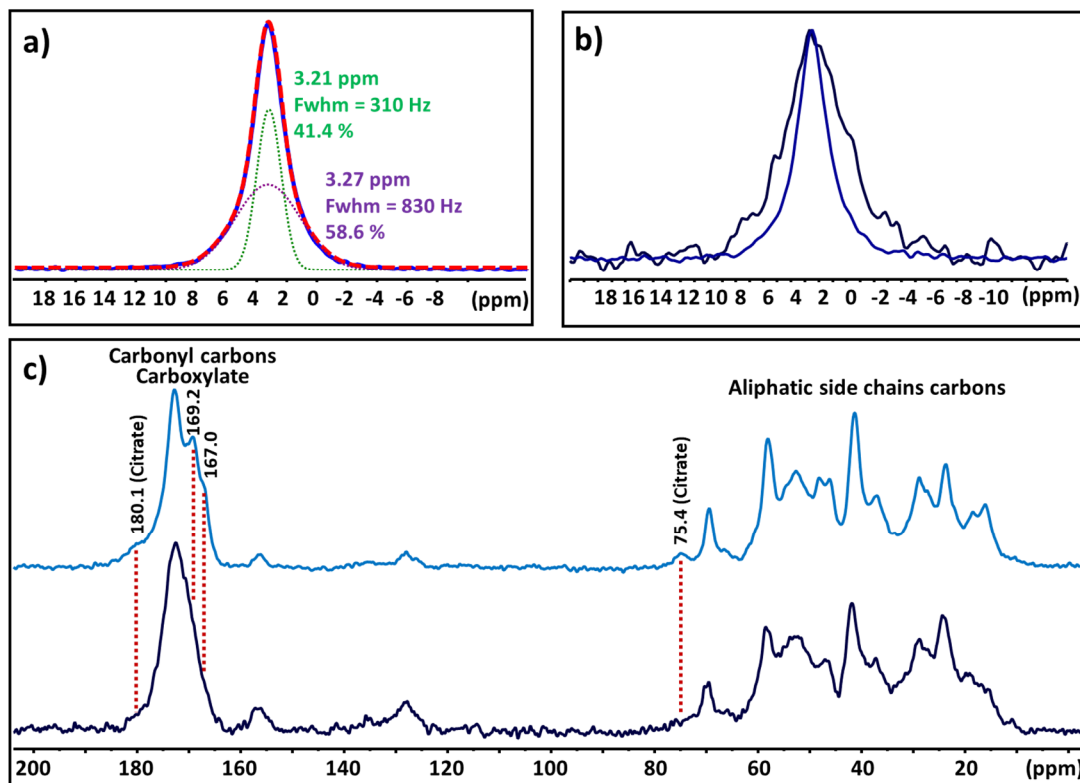
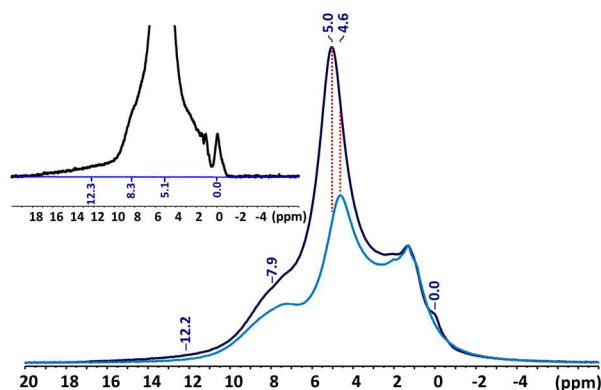


Fig. 2. 1D MAS NMR spectra: (a) ^{31}P ($\nu_r = 60$ kHz, relaxation delay 600 s) of Hu-dentin (blue) with spectral deconvolution (red). (b) ^{31}P CP ($\nu_r = 60$ kHz) of Hu-dentin with contact time of 10 ms (blue) and

155 of 0.2 ms (black), with intensities normalized for their comparison. (c) ^{13}C quantitative CP ($\nu_r = 12$ kHz) of (top) Hu-dentin and (bottom) demineralized dentin (Dm-dentin).

The ^1H single-pulse MAS spectrum of Hu-dentin is very complex even at very fast MAS (Fig. 3, black) because it consists of the superposition of signals of many species. One of the main contributions at *ca* 5 ppm comes from water molecules found in different environments: free (or mobile) and weakly or strongly bound to the different components of the dentin. The majority of water molecules are found in the inorganic ACP phase, in the collagen network or at the organic/inorganic interface [20,25,29,30]. In addition to the strong water signal, broad ^1H peaks between 1 to 9 ppm originates from amide and aliphatic protons of the organic matrix (mainly collagen proteins) [23]. Then, two other types of protonated species have been identified. The first one is the signal coming from the hydroxyl groups of the HAp crystallites around 0 ppm [24,48]. The second one is a broad HPO_4^{2-} ion signal with chemical shift above 7 ppm [11,15,16]. The precise ^1H chemical shift of each phosphonate ion is dictated by its degree of hydrogen bonding to neighboring O atoms: the chemical shift of an H-bonded $\text{OH}\cdots\text{O}$ group increases while the $\text{H}\cdots\text{O}$ distance decreases [49,50]. This also applies to water molecules or hydroxyl groups with a chemical shift distribution also dependent on the hydrogen bond strength. Other less well characterized peaks in the 0.9-2.0 ppm area have been described. They are either assigned to aliphatic fatty molecules [25] or to H_2O molecules that terminate the HAp OH channels [51] or to hydrogen bonded hydroxyl groups [52] notably close to carbonate ions [25,53].



175 **Fig. 3.** ^1H MAS NMR spectra ($\nu_r = 60$ kHz, relaxation delay 10s) of Hu-dentin (black) and Dm-dentin (blue). Insert: spectral difference between the two spectra.

The main objective of this study was to obtain a better attribution of the ^1H signals of the dentin. For that, we have prepared a first sample of demineralized dentin (Dm-dentin) by etching the Hu-dentin powder with phosphoric acid. After rinsing, no ^{31}P signal could be observed for Dm-dentin confirming the disappearance of the mineral phase. The ^{13}C CPMAS (Fig. 2c bottom) spectrum of the Dm-dentin mainly corresponds to the spectrum of collagen fibers (plus non-collagenous macromolecules in minor amounts). However, the ^{13}C signal of the Dm-dentin sample are broader than the ones of the Hu-dentin sample (notably the methyl group ones around 20 ppm). This indicates a higher structural disorder for the collagen in the Dm-dentin than in the Hu-dentin associated to the removal of the apatitic platelets and also possibly to a partial dehydration of the collagen [7]. It should be noted that the carbonate and citrate ions

signals (at 180.1, *ca.* 168 and 75.4 ppm) are absent confirming their link with the inorganic phase. The ^1H signals of Dm-dentin (Fig. 3, blue) around 8 ppm and between 1 and 5 ppm correspond to the amide and aliphatic side chain hydrogens of collagen, respectively. A strong signal at 4.6 ppm is also observed indicating the presence of water molecules bound to the organic phase. The weakly bound water molecules can be removed by vacuum drying (Fig. 4a) but a residual signal of more strongly bound water molecules may overlapped with the one of aliphatic protein hydrogens ($\text{H}_\alpha/\text{H}_\beta$).

To better characterize the organic phase of the Dm-dentin, ^1H MAS NMR experiments were performed with dipolar filtering (DF-SE, Fig. 4b,c,d) [37]. A short filtering time (0.76 ms) allows for the elimination or reduction of signal with strong H-H dipolar couplings (rigid species with short H-H distance) while a long filtering time (6.0 ms) allows for the edition of signal with weak H-H dipolar couplings (mobile species or isolated H atoms) [26]. The short filtering time leads to a rapid decrease of the collagen and water signals (comparison of black and blue spectra in Fig. 4b). After the short filtering time (Fig. 4c), a strong signal at 4.6 ppm is still observed that is a superposition of the residual signal of water molecules with low mobility (interfacial water or water molecules moderately bound to collagen) and the signal of mobile water molecules. This signal is strongly reduced by vacuum drying. The signals of mobile species appear distinctly with the long filtering time (Fig. 4d). A residual signal at 4.8 ppm is detected that can be assigned to a pool of mobile water molecules in the organic phase (free water) also removed by vacuum drying. Furthermore, narrow signals between 0.9 and 2.0 ppm are clearly observed.

205

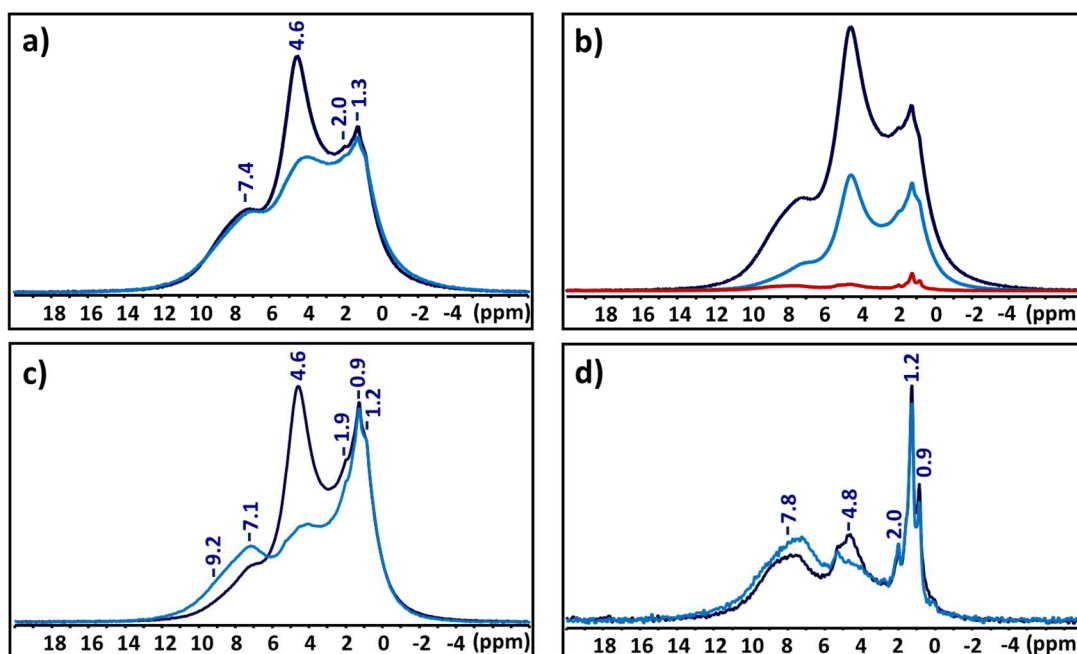


Fig. 4. ^1H MAS NMR spectra ($\nu_r = 60$ kHz, relaxation delay 10s) of (a) Dm-dentin before (black) and after (blue) vacuum drying, of (b) Dm-dentin (black) with short (0.76 ms, blue) and long (6 ms, red) dipolar filtering time (DF-SE), of Dm-dentin before (black) and after (blue) vacuum drying with short 0.76 ms (c) and long 6 ms (d) filtering time.

210

As the inorganic phase is absent in the demineralized dentin and these signals are not affected by the vacuum drying, they can be assigned to mobile aliphatic fatty molecules. The ^1H DF-SE MAS also highlights the structuring role of water molecules in collagen fibers [19,20,32]. Comparison of ^1H DF-SE MAS with short filtering time of Dm-dentin with or without vacuum drying (Fig. 4c) evidences a slower dipolar relaxation of the amide hydrogens (at *ca.* 8 ppm) following the reduction in the number of H-bonded water molecules in the collagen helical structure. This effect can be due to an increase of the dynamic behaviour of amide groups linked to a reduction of structural water molecules.

The same vacuum drying and dipolar filtering experiments were realized on the Hu-dentin sample. The vacuum drying on the Hu-dentin (Fig. 5) has the effect of removing many water molecules. Most of them have a typical signal around 5.0 ppm but some of them have more or less shielded signals (between 1.4 to 9 ppm). This result is clearly different from the one observed for the organic phase alone where only the signal centered at 4.6 ppm strongly decreased. It indicates that a high proportion of water molecules is linked to the inorganic phase. The signal above 5 ppm can be assigned to water molecules involved in strong hydrogen bonding while signals less than 4 ppm are associated to isolated water molecules involved (or not) in weak hydrogen bonds. Notably, it has been proposed that H_2O molecules close to the HAp OH channels have a signal between 1.2 and 2.0 ppm [25,51]. After vacuum drying the center of gravity of the water signal shifted to 4.6 ppm as for the organic phase (Fig. 5a). It can also be noted that the hydroxyl signal of HAp (at 0 ppm) is barely affected by the vacuum drying. These hydroxyl groups seem highly trapped in the apatite phase. The dipolar filtering spectra (Fig. 5b,c,d) display similarities to those of the organic part: rapid decrease of collagen and water signals and a slower dipolar relaxation of amide hydrogens after drying (Fig. 5c). Also, a pool of mobile water molecules can be detected at 4.9 ppm after the long filtering time (Fig. 5d). Furthermore, the HAp hydroxyl signal at 0 ppm decreases at a slower rate than the other Hu-dentin signal because of their very weak H-H dipolar couplings [26,48]. A notable difference with the results for the Dm-dentin concerns the signals of mobile species between 0.9 and 2.0 ppm. Some signals were observed for the Hu-dentin sample in this area with the long filtering time but they disappeared after vacuum drying (Fig. 5d). This result is more in line with an assignment of 0.9-2.0 ppm signal to H_2O molecules at the HAp OH channels. A possible explanation for this difference is contamination of the Dm-dentin sample by a small amount of grease during the additional steps requiring for its preparation or its transfer into the MAS rotor (DM-dentin sample was in the form of a sticky gel).

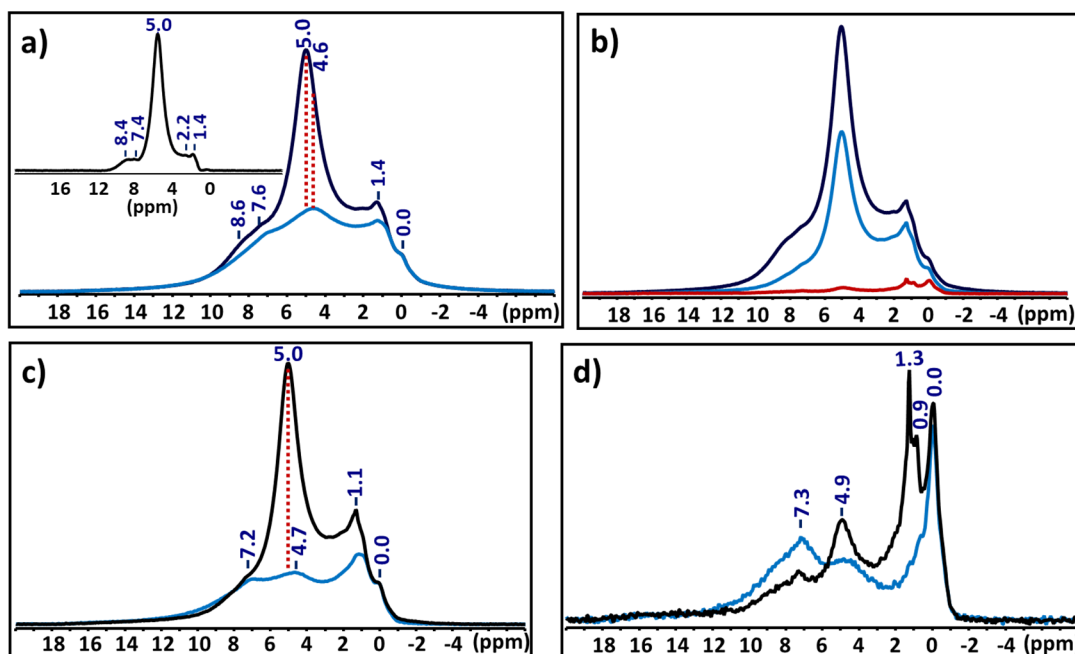


Fig. 5. ^1H MAS NMR spectra ($\nu_r = 60$ kHz, relaxation delay 10s) of (a) Hu-dentin before (black) and after (blue) vacuum drying (Insert: spectral difference between the two spectra), of (b) Hu-dentin (black) with short (0.76 ms, blue) and long (6 ms, red) dipolar filtering time (DF-SE), of Hu-dentin before (black) and after (blue) vacuum drying with short 0.76 ms (c) and long 6 ms (d) filtering time.

245

To obtain additional information on the ^1H signals of the inorganic phase, we performed 1D $^1\text{H}/^{31}\text{P}$ double cross polarization (DCP) NMR experiment (Fig. 6a) [16,38]. The double CP transfer conducted in a “there-and-back” manner ($^1\text{H} \rightarrow ^{31}\text{P} \rightarrow ^1\text{H}$) provides ^{31}P -filtered ^1H NMR spectra of Hu-dentin. Short CP times should favor observation of ACP hydrogens while long CP times should give stronger HAp H signals because of their different cross-polarization dynamics (*vide supra*). The $^1\text{H}/^{31}\text{P}$ DCP spectrum with short CP times (3 ms - 0.2 ms, Fig. 6a blue) presents mostly signal between 5.5 and 17 ppm confirming the presence of structural water molecules and acidic HPO_4^{2-} ion in the ACP phase. Use of longer CP times (6 ms - 2 ms, Fig. 6a black) shows a strong enhancement of the HAp hydroxyl signal (at 0 ppm) and of more mobile water molecules (around 5.3 ppm). As this pool of water molecules is observed with the cross-polarization method this indicates they have significant dipolar coupling with ^{31}P nuclei and thus a reduced mobility. It corresponds in part to water signals that disappear in the dipolar filtering experiment with the short filtering time. In contrast, the H resonances between 0.8 to 4.5 ppm of aliphatic groups, isolated water molecules and hydrogen bond hydroxyl groups, have weak intensities in the $^1\text{H}/^{31}\text{P}$ DCP spectrum. These small magnetization transfers with ^{31}P nuclei suggest species that are either mobile and/or remote from phosphate groups. 2D $^1\text{H}/^{31}\text{P}$ HETCOR spectrum (Fig. 6b) are in agreement with the $^1\text{H}/^{31}\text{P}$ DCP results. However, it does not provide a better ^1H characterization due to the strong overlapping of the HAp and ACP ^{31}P signals associated with wide distribution of hydrogen chemical environments and noise increase related to the acquisition of the bi-dimensional experiment. In order to compare the H signals of the organic and inorganic phase of the Hu-dentin a 1D $^1\text{H}/^{13}\text{C}$ DCP spectrum (3 ms - 2 ms) was acquired (Fig. 6c). Signal associated mostly with collagen protein hydrogens

260

265

can be seen between 1 and 9 ppm. In addition, a weak signal of acidic H that could be assigned to bicarbonate HCO_3^- ions is detected around 13.6 ppm. [54].

270

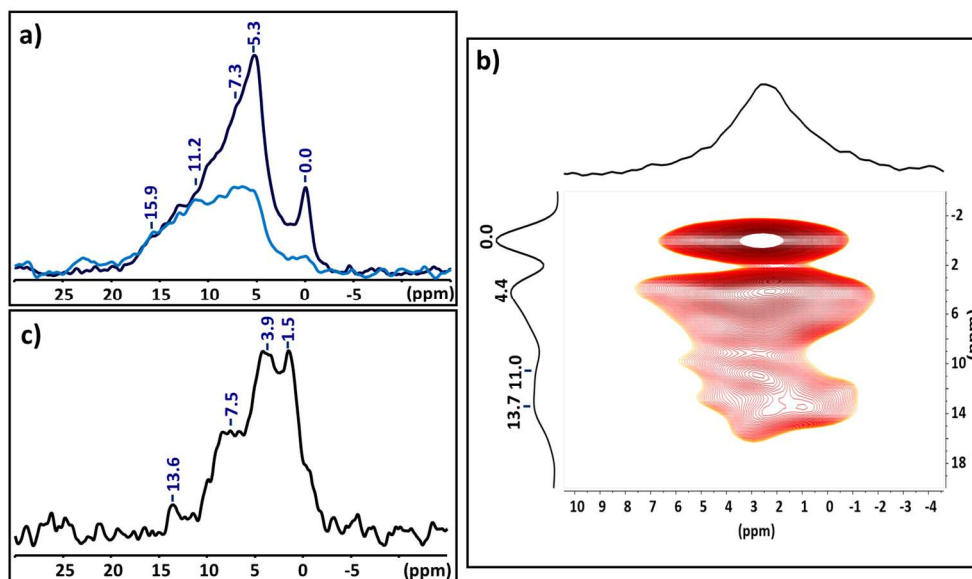


Fig. 6. MAS NMR spectra ($\nu_r = 60$ kHz) of Hu-dentin: (a) $^1\text{H}/^{31}\text{P}$ double cross polarization (DCP) with long (6 ms - 2 ms, black) and short (3 ms - 0.2 ms, blue) CP times. (b) 2D $^1\text{H}/^{31}\text{P}$ HETCOR (contact time 2 ms). (c) $^1\text{H}/^{13}\text{C}$ DCP (contact times 3 ms - 2 ms).

275

The next characterization step of the ^1H signals was to perform 2D Single Quantum-Single Quantum (SQ-SQ, NOESY) and Double Quantum-Single Quantum (DQ-SQ) MAS NMR experiments. The DQ-MAS spectra of the Hu-dentin and of Dm-dentin (Fig. 7) were strongly similar. DQ-spectrum makes it possible to identify pairs of close hydrogens from the dipolar-coupled network (rigid species). The DQ spectra of both samples are dominated by the correlations between H of collagen. However, the DQ signal assigned mostly to collagen $\text{H}_\alpha/\text{H}_\alpha$ and $\text{H}_\alpha/\text{H}_\beta$ correlations at 4.4/8.8 ppm for Dm-dentin was shifted to 5.0/9.1 ppm for Hu-dentin. This high frequency shift can be related to an additional contribution of water hydrogen signals with low mobility. Moreover, self DQ correlations for Hu-dentin signals detected in the 5.5-6.8 ppm range that were absent for Dm-dentin, can be assigned to structural water molecules in the ACP phase. It is also interesting to note that a self DQ signal around 7.0 ppm is observed in both samples. This DQ correlation was also detected by Sinsha *et al.* for native collagen but disappears for dehydrated collagen [32]. We assigned this DQ signal to water molecules tightly bound to collagen through strong hydrogen bonds. Good candidates for such structural water molecules are the ones of interchain water bridges that stabilized the tropocollagen helical structure [23].

280

285

290

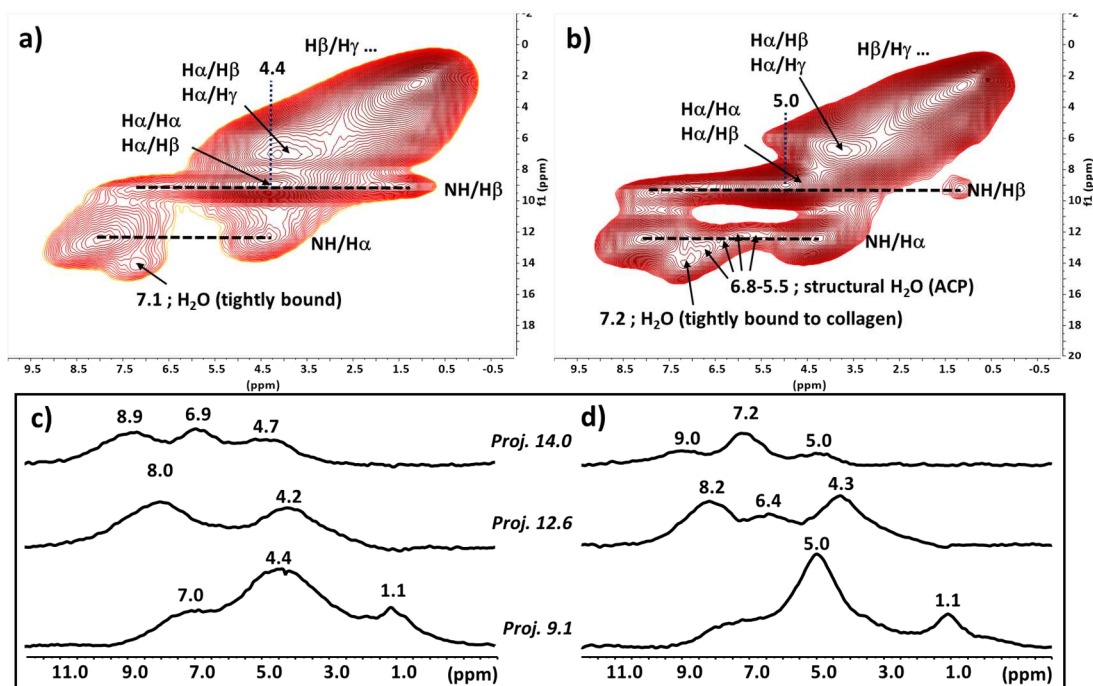


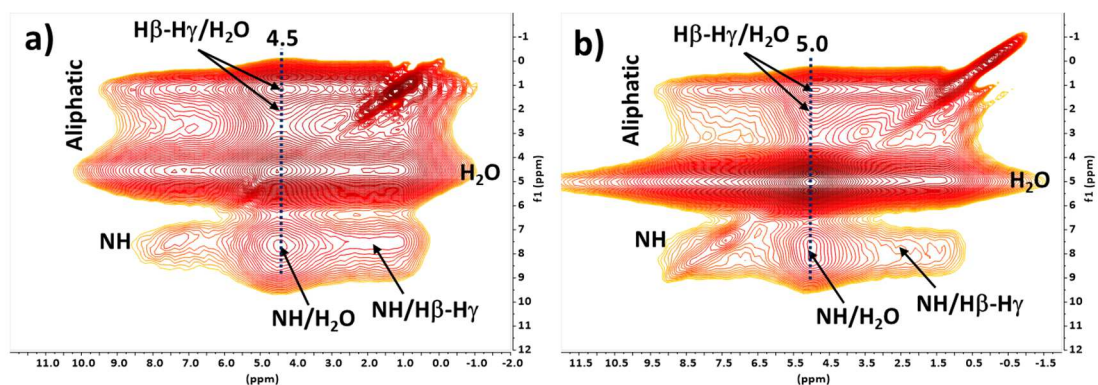
Fig. 7. 2D ^1H DQ-MAS NMR spectrum ($\nu_r = 60$ kHz) of (a,c) Dm-dentin and (b,d) Hu-dentin with f_1 projections at 9.1, 12.6 and 14.0 ppm.

295 The SQ-SQ (NOESY) NMR spectra are also very similar for both Hu-dentin and Dm-dentin samples (Fig. 8). One set of correlations involved dipolar transfer of magnetization (due to spatial proximity) between the H of collagen (NH, H_α , H_β , H_γ ...). However, the stronger SQ correlations are seen between the water hydrogens (between 4.5 to 5 ppm) and the NH (at *ca.* 8 ppm) and H_β , H_γ of collagen (between 2.2 and 1.2 ppm). The same strong water-collagen SQ correlations were observed by Ramamoorthy *et al.*

300 on bone [32]. The water-amide correlation was attributed to water molecules strongly bonded to collagen helices and the water- H_β , H_γ correlation to polar (van der Waals) interactions between mobile water and collagen side chains. However, the fact that the water signal of the organic phase around 5 ppm disappears almost completely with vacuum drying (Fig. 4a) and its low chemical shift does not seem to be in agreement with an expected signal of structural water molecules inside the collagen helices. We propose that the water-amide SQ-SQ correlation is associated with water molecules moderately hydrogen

305 bonded to amide groups at the tropocollagen helices surface. As for 1D ^1H and 2D DQ spectra, the water SQ correlation signals is high frequency shifted for Hu-dentin compared to Dm-dentin (5.0 vs 4.5 ppm). This indicates that for Hu-dentin the high frequency part of the water signal (between 5 to 4.5 ppm) is also in close contact with the collagen phase. It can be concluded that the Hu-dentin water signal centered

310 at 5.0 ppm corresponds mostly to water molecules in close contact to collagen (between the tropocollagen helices or at the organic-inorganic interface). It is also interesting to note that for both SQ-SQ and DQ-SQ, correlation signals are absent for HPO_4^{2-} and HAp hydroxyl hydrogens indicating that these species are more isolated.



315

Fig. 8. 2D ^1H SQ-MAS (NOESY) NMR spectrum ($\nu_r = 60$ kHz, mixing time 18 ms) of (a) Dm-dentin and (b) Hu-dentin.

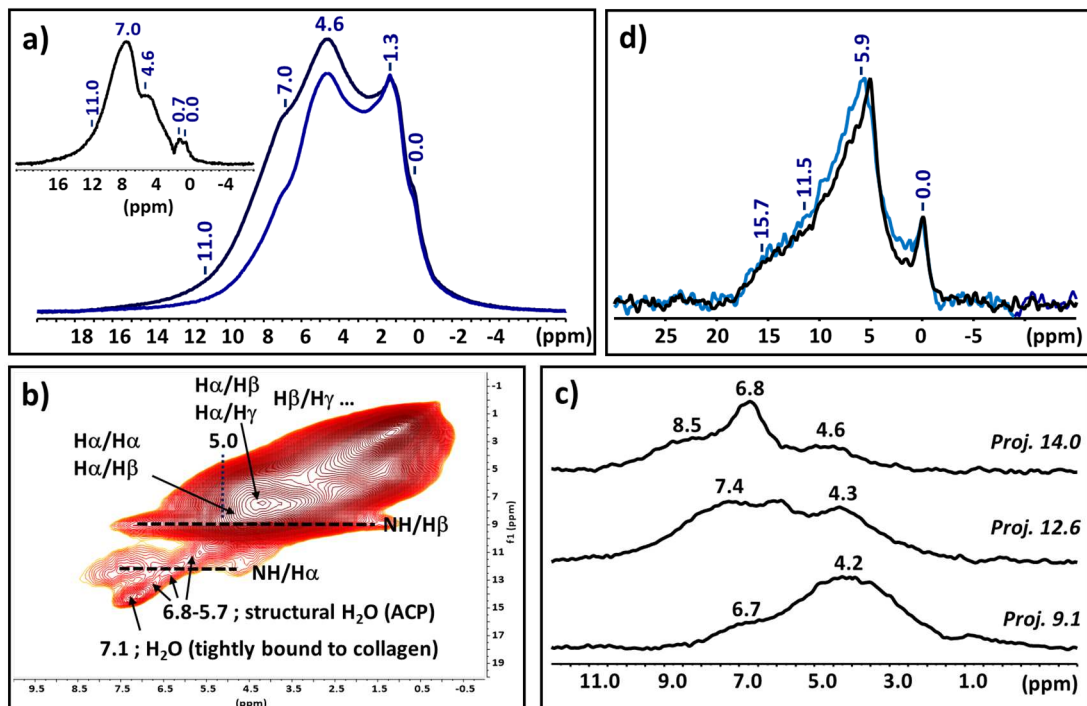
320 These assignments were confirmed by exposing the Hu-dentin sample to D_2O for 24 h in order to exchange labile hydrogens by deuteriums followed by vacuum drying (Fig. 9). This protocol allows the identification of the H of dentin that can exchange slowly with the H of free water molecules. Above all, signals of amide and water hydrogens involved in weak hydrogen bond should disappear (or be strongly reduced) by deuterium exchange while strongly H-bonded ones could be preserved. Comparison of the ^1H MAS spectra of vacuum dried Hu-dentin with the one of Hu-dentin exposed to D_2O for 24 h followed by vacuum drying evidences a strong decrease of the signal centered around 7.0 and 4.6 ppm (Fig. 9a). The last one corresponds to a part of the water molecules moderately bound to collagen assigned above. The first one could be due to deuteration of amide H of collagen and/or structural water. Additional information is provided by DQ experiment on deuterated Hu-dentin sample (Fig. 9b,c). The DQ signals assigned to NH/ H_α correlation are strongly reduced and shifted (from correlation between H pairs 4.4/8.0 ppm to 4.3/7.4 ppm) indicating that most amide H were deuterated. On the contrary, those of structural water in the 5.7–7.2 ppm range are more resistant to deuteration because they are involved in stronger H-bonds. Another DQ correlation that is strongly reduced after deuterium exchange is the one at 5.0/9.1 ppm observed for Hu-dentin (Fig. 7b) associated with water H. We can also note that the 4.4/8.8 ppm DQ signal for Dm-dentin assigned to $\text{H}_\alpha/\text{H}_\alpha$ and $\text{H}_\alpha/\text{H}_\beta$ pairs (Fig. 7a) is much more intense than the one in the same area for deuterated Hu-dentin (Fig. 9b). Since, collagen H_α and H_β hydrogens should not experience deuterium exchange and so no decrease of their DQ signal, the signal decay in this region can only be attributed to the deuteration of the water molecules. This confirms that water molecules for Dm-dentin with ^1H signal around 4.4-4.6 ppm have a labile nature and are not strongly bonded inside the collagen helices. The Hap H hydroxyl are only weakly affected by deuterium exchange with a small decrease of the signal around 0-0.7 ppm (Fig. 9a). A signal decrease is observed on the ^1H spectrum after exposition to D_2O in the 10-14 ppm area corresponding to labile acidic H. However, the $^1\text{H}/^{31}\text{P}$ DCP experiment (Fig. 9d) shows that the signal of rigid HPO_4^{2-} groups is mainly retained. This decrease may be associated to some labile phosphonate hydrogens with the weakest H-bonds and other labile acidic H resonances.

325

330

335

340



345

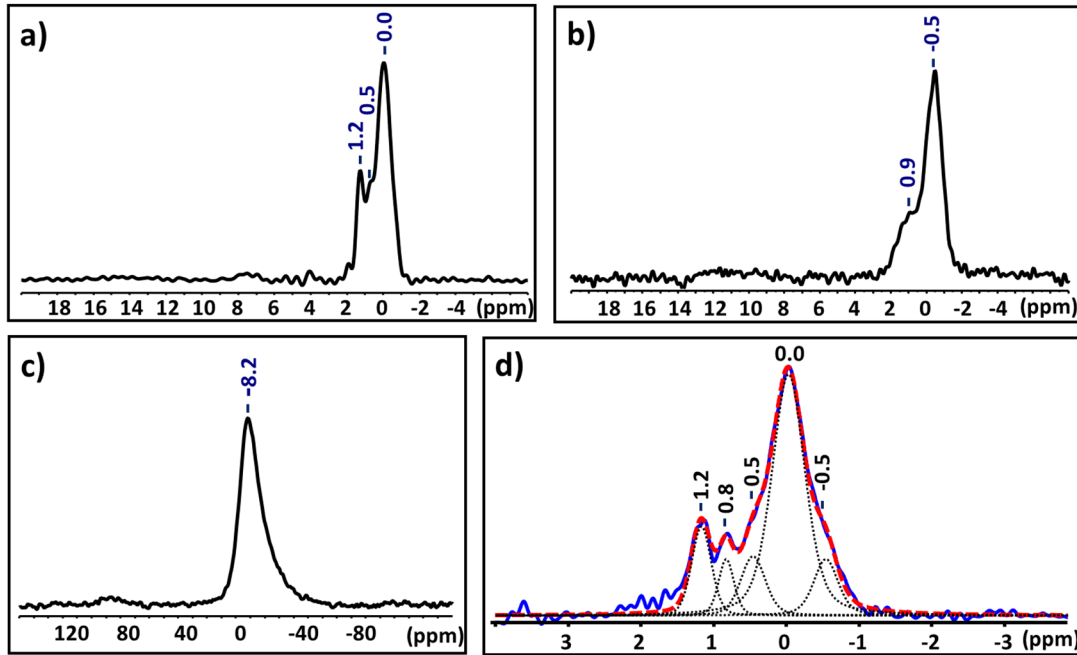
Fig. 9. MAS NMR spectra ($\nu_r = 60$ kHz): (a) ^1H (relaxation delay 10s) after 1 h of vacuum drying of Hu-dentin before (black) and after (blue) exposition to D_2O for 24 h (Insert: spectral difference between the two spectra), (b) 2D ^1H DQ of dried deuterated Hu-dentin with (c) f1 projections at 9.1, 12.6 and 14.0 ppm, (d) $^1\text{H}/^{31}\text{P}$ DCP (contact times 6 ms – 2 ms) of Hu-dentin before (black) and after (blue) deuteration and drying.

350

Finally, we also performed 1D ^1H - ^{43}Ca and ^1H - ^{23}Na D-HMQC [40] MAS experiments on the Hu-dentin sample (Fig. 10). ^1H - ^{43}Ca D-HMQC has been used by Smith *et al.* to study HAp before and after heating to 1150 °C (oxy-Hap) [27]. $^1\text{H}/^{43}\text{Ca}$ correlations were observed for H signal at 0 ppm (HAp hydroxyl) and at *ca.* 1.0 and 1.4 ppm. These two last signals were attributed to hydroxyl groups involved in hydrogen bonds as a result of the presence of O^{2-} and oxygen vacancies in oxy-HAp. The 1D ^1H - ^{43}Ca D-HMQC spectrum of Hu-dentin (Fig. 10a) shows three H signals between 0 to 1.2 ppm in line with the result of Smith *et al.*. The same group in another study also used ^1H - ^{23}Na D-HMQC to analyze equine bone and bovine teeth [28]. 2D ^1H - ^{23}Na correlations were detected between ^{23}Na at -1.7 ppm and hydroxyl close to 0 ppm (the exact ^1H chemical shift value was not provided). The ^{23}Na MAS spectrum of Hu-dentin (Fig. 10c) shows a broad signal centered at -8.2 ppm. ^{23}Na is a quadrupolar nucleus and its exact chemical shift depends on the value of its quadrupolar coupling. It has to be determined through ^{23}Na MQMAS experiment at different magnetic fields. However, our dentin ^{23}Na signal is clearly similar to the one published for bovine teeth. The 1D ^1H - ^{23}Na D-HMQC spectrum of Hu-dentin shows two signals at -0.5 and 0.9 ppm (Fig. 10b) in agreement with the 2D correlation for bovine teeth. The fact that the hydroxyl signal around 0 ppm is more complex than a single resonance has already been reported [15,26]. By conducting a ^1H DF-SE experiment with a very long filtering time of 23 ms (Fig. 10d), we were able to observe selectively the hydroxyl signals around 0 ppm. This signal has to be deconvoluted with three contributions at -0.5, 0.0 and 0.5 ppm plus two other more high frequency signals at 1.2 and 0.8 ppm. From our study and previous results of the literature presented above, we propose assigning

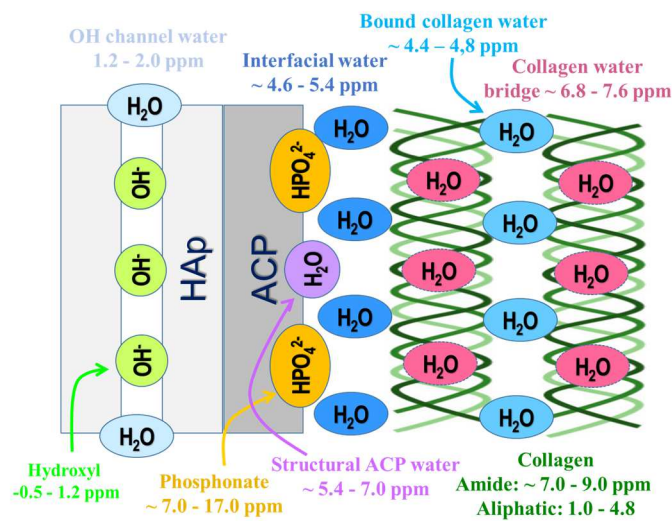
370

these five signals to hydroxyl groups of the apatite structure (HAp and NS-HAp) close to the different metal cations (Ca^{2+} , Na^+ ...) but also to carboxylate CO_3^{2-} and O^{2-} ions and to oxygen vacancies.



375 **Fig. 10.** 1D MAS NMR spectra of Hu-dentin: 1D $^1\text{H}/^{43}\text{Ca}$ (a) and $^1\text{H}/^{23}\text{Na}$ (b) D-HMQC ($\nu_r = 12$ kHz),
 (c) 1D ^{23}Na ($\nu_r = 12$ kHz, relaxation delay 1s), (d) ^1H DF-SE ($\nu_r = 60$ kHz) with very long 23 ms filtering
 380 time (in blue) with spectral deconvolution (in red).

The combination of all the ^1H results reported in this study in combination with previous results of the literature allows us to propose a schematic view of the main hydrogenated dentin species (Fig. 11) with their NMR characteristics resumed in Table 1.



385 **Fig. 11.** Schematic view of the main hydrogenated dentin species with their ^1H chemical shift range.

Table 1. Hydrogenated dentin species with their estimated chemical shift range, the ssNMR experiments allowing their identification and their sensitivity to vacuum drying and deuterium exchange.

Hydrogenated species	¹ H chemical shift range (ppm)	ssNMR edition method	Vacuum drying	Deuterium exchange
Hydroxyl (HAp, NS-HAp)	-0.5 – 1.2	DF-SE (long filtering time) ¹ H/ ³¹ P DCP (long CP times) ¹ H/ ⁴³ Ca and ¹ H/ ²³ Na 1D HMQC	No	No
OH channel water (HAp, NS-HAp)	1.2 – 2.0	DF-SE (long filtering time)	Yes	Yes
Aliphatic side chains (Collagen)	1.0 – 4.8	¹ H/ ¹³ C DCP ¹ H DQ-SQ MAS	No	No
Moderately bound collagen water	4.4 – 4.8	DF-SE (short filtering time) ¹ H SQ-SQ MAS	Yes	Yes
Free water	4.7 - 5.2	DF-SE (long filtering time)	Yes	Yes
Interfacial water	4.6 – 5.4	DF-SE (short filtering time) ¹ H SQ-SQ MAS ¹ H/ ³¹ P DCP (long CP times)	Yes	Yes
Structural ACP water	5.4 – 7.0	¹ H/ ³¹ P DCP (short CP times) ¹ H DQ-SQ MAS	No	No
Tropocollagen water bridges	6.8 - 7.6	¹ H DQ-SQ MAS	No	No
Amide (Collagen)	7.0 – 9.0	¹ H/ ¹³ C DCP ¹ H DQ-SQ MAS	No	Yes
Phosphonate ions (ACP)	7.0 - 17.0	¹ H/ ³¹ P DCP (short CP times)	No	No
Bicarbonate ions	13.0-14.0	¹ H/ ¹³ C DCP	na	na

na: not assessed.

390 4. Conclusions

This work shows that selective editions of ¹H MAS NMR signals of dentine components, according to their location and dynamic behaviour, can be carried out. It allows us to propose the most detailed ¹H NMR signal assignment of dentine to date. Various hydrogenated species like water molecules, HPO₄²⁻ and OH⁻ groups, either bound to the organic phase of proteins or linked to the mineral calcium phosphate solids and with different local mobilities, could be highlighted. Most of the edited NMR spectra are recorded as fast 1D experiments using homo- and hetero-nuclear dipolar coupling filters. ¹H ssNMR assignment is also facilitated by simple sample modifications: vacuum drying, deuterium exchange and demineralization. This set of ssNMR experiments constitutes an important toolbox to define the different components, particularly water, of apatitic materials. It enables a fine monitoring of their evolutions according to physical or chemical modifications and represents an important advancement in understanding the complex nature of apatitic materials.

Acknowledgements

The financial support from the European Regional Development Fund (ERDF/FEDER) of the
405 European Commission is kindly acknowledged.

References

- [1] G.W. Marshall, S.J. Marshall, J.H. Kinney, M. Balooch, The dentin substrate: structure and properties related to bonding, *J. Dent.* 25 (1997) 441-58.
- 410 [2] M. Goldber, A.B. Kulkarni, M. Young, A. Boskey, Dentin: structure, composition and mineralization, *Front Biosci (Elite Ed)* 3 (2011) 711-735.
- [3] C. Combes, S. Cazalbou, C. Rey, Apatite Biominerals. *Minerals* 6 (2016), 34.
- [4] J. de Dios Teruel, A. Alcolea, A. Hernández, A.J.O. Ruiz, Comparison of chemical composition of enamel and dentine in human, bovine, porcine and ovine teeth. *Arch. Oral Biol.* 60 (2015)
415 768–775.
- [5] N. Vandecandelaère , E. Champion , F. Rossignol , A. Navrotsky , D. Grossin , M. Aufray , S. Rollin-Martinet , C. Drouet , C. Rey ,Nanocrystalline apatites: the fundamental role of water, *Am. Mineral.* 103 (2018) 550–564.
- [6] M.J. Duer, The contribution of solid-state NMR spectroscopy to understanding
420 biomineralization: atomic and molecular structure of bone, *J. Magn. Reson.* 253 (2015) 98–110.
- [7] K.H. Mroue, A. Viswan, N. Sinha, A. Ramamoorthy, Solid-state NMR spectroscopy: the magic wand to view bone at nanoscopic resolution, *Annu. Rep. NMR Spectrosc.* 92 (2017) 365–413.
- [8] C. Gervais, C. Bonhomme, D. Laurencin, Recent directions in the solid-state NMR study of synthetic and natural calcium phosphates, , *Solid State Nucl. Magn. Reson.* 107 (2020) 101663.
- 425 [9] J. Kolmas, W. Kolodziejwski, Concentration of hydroxyl groups in dental apatites: a solid-state ^1H MAS NMR study using inverse $^{31}\text{P} \rightarrow ^1\text{H}$ cross-polarization, *Chem. Comm.* 42 (2007) 4390-4392.
- [10] T.G.Nunes, M. Polido, A. Amorim, S. G. Nunes, M. Toledano, Multinuclear magnetic resonance studies on the chemical interaction of a self-etching adhesive with radicular and coronal human
430 dentin. *J. Mater. Sci. Mater. Med.* 18 (2007) 2093–2099.
- [11] S.-J. Huang, Y.-L. Tsai, Y.-L. Lee, C.-P. Lin, J.C.C. Chan, Structural model of rat dentin revisited, *Chem. Mater.* 21 (2009) 2583–2585.
- [12] Y.-L. Tsai, M.-W. Kao, S.-J. Huang, Y.-L. Lee, C.-P. Lin, J.C.C. Chan, Characterization of Phosphorus Species in Human Dentin by Solid-State NMR. 25 (2020) *Molecules* 196.
- 435 [13] Y. Wu, J.L. Ackerman, H.-M. Kim, C. Rey, A. Barroug, M.J. Glimcher, Nuclear magnetic resonance spin-spin relaxation of the crystals of bone, dental enamel, and synthetic hydroxyapatites, *J. Bone Miner. Res. Off. J. Am. Soc. Bone Miner. Res.* 17 (2002) 472–480.

- [14] W. Kolodziejski, Solid-state NMR studies of bone, in: *New Techniques in Solid-State NMR*, Springer Berlin Heidelberg, 246 (2005) 235–270.
- 440 [15] S. Von Euw, Y. Wang, G. Laurent, F. Babonneau, N. Nassif, T. Azaïs, Bone mineral: new insights into its chemical composition. *Sci Rep* 9 (2019) 8456.
- [16] S. Von Euw, W. Ajili, T.-H.-C. Chan-Chang, A. Delices, G. Laurent, F. Babonneau, N. Nassif, T. Azaïs, Amorphous surface layer versus transient amorphous precursor phase in bone – a case study investigated by solid-state NMR spectroscopy, *Acta Biomater.* 59 (2017) 351–360.
- 445 [17] K. Beshah, C. Rey, M.J. Glimcher, M. Schimizu, R.G. Griffin, Solid state carbon-13 and proton NMR studies of carbonate-containing calcium phosphates and enamel, *J. Solid State Chem.* 84 (1990) 71–81.
- [18] C. Jaeger, N. S. Groom, E. A. Bowe, A. Horner, M. E. Davies, R. C. Murray, M. Duer, Investigation of the nature of the protein-mineral interface in bone by solid-state NMR, *Chem. Mater.* 17 (2005) 3059-3061.
- 450 [19] P. Zhu, J. Xu, N. Sahar, M. D. Morris, D.H. Kohn, A. Ramamoorthy, Time-resolved dehydration-induced structural changes in an intact bovine cortical bone revealed by solid-state NMR spectroscopy, *J. Am. Chem. Soc.* 131 (2009) 17064–17065.
- [20] R.K. Rai, N. Sinha, Dehydration-induced structural changes in the collagen– hydroxyapatite interface in bone by high-resolution solid-state NMR spectroscopy, *J. Phys. Chem. C* 115 (2011) 14219–14227.
- 455 [21] Y.Y. Hu, A. Rawal, K. Schmidt-Rohr, Strongly bound citrate stabilizes the apatite nanocrystals in bone, *Proc. Natl. Acad. Sci. U S A.* 107 (2010) 22425–22429.
- [22] E. Davies, K.H. Müller, W.C. Wong, C.J. Pickard, D.G. Reid, J.N. Skepper, M.J. Duer, Citrate bridges between mineral platelets in bone, *Proc. Natl. Acad. Sci. U.S.A.* 111 (2014) E1354–E1363.
- 460 [23] K.H. Mroue, Y. Nishiyama, M. Kumar Pandey, B. Gong, E. McNerny, D.H. Kohn, M.D. Morris, A. Ramamoorthy, Proton-detected solid-state NMR spectroscopy of bone with ultrafast magic angle spinning, *Sci. Rep.* 5 (2015) 11991.
- 465 [24] G. Cho, Y. Wu, J. L. Ackerman, Detection of hydroxyl ions in bone mineral by solid-state NMR spectroscopy. *Science* 300 (2003) 1123-1127.
- [25] E. E Wilson, A. Awonusi, M. D Morris, D. H Kohn, M.M.J. Tecklenburg, L.W. Beck, Three structural roles of water in bone observed by solid-state NMR, *Biophys. J.* 90 (2006) 3722–3731.
- 470 [26] A. Kaflak, S. Moskalewski, W. Kolodziejski, The solid-state proton NMR study of bone using a dipolar filter: apatite hydroxyl content versus animal age. *RSC Adv.* 9 (2019) 16909-16918
- [27] A. Wong, D. Laurencin, R. Dupree, M. E. Smith, Two-dimensional ^{43}Ca - ^1H correlation solid-state NMR spectroscopy, *Solid State Nucl. Magn. Reson.* 35 (2009) 32–36.
- 475 [28] D. Laurencin, A. Wong, W. Chrzanowski, J.C. Knowles, D. Qiu, D.M. Pickup, R.J. Newport, Z. Gan, M.J. Duer, M.E. Smith, Probing the calcium and sodium local environment in bones and

- teeth using multinuclear solid state NMR and X-ray absorption spectroscopy, *Phys. Chem. Chem. Phys.* 12 (2010) 1081-1091.
- [29] F. W. Wehrli, M. Fernández-Seara, Nuclear magnetic resonance studies of bone water. *Ann. Biomed. Eng.* 33 (2005) 79–86.
- 480 [30] E. E Wilson, A. Awonusi, M. D Morris, D. H Kohn, M.M.J. Tecklenburg, L.W. Beck, Highly ordered interstitial water observed in bone by nuclear magnetic resonance, *J. Bone Miner. Res.* 20 (2005) 625–634.
- [31] Y. Wang, S. Von Euw, F.M. Fernandes, S. Cassaignon, M. Selmane, G. Laurent, G. Pehau-Arnaudet, C. Coelho, L. Bonhomme-Coury, M.-M. Giraud-Guille, F. Babonneau, T. Azaïs, N.
485 Nassif, Water-mediated structuring of bone apatite, *Nat. Mater.* 12 (2013) 1144–1153.
- [32] R.K. Rai, C. Singh, N. Sinha, Predominant role of water in native collagen assembly inside the bone matrix, *J. Phys. Chem. B* 119 (2015) 201–211.
- [33] S. Elfersi, G. Grégoire, P. Sharrock, Characterization of sound human dentin particles of sub-millimeter size, *Dental Materials* 18 (2002) 529-534.
- 490 [34] G. Grégoire, P. Sharrock, M.P. Lacomblet, B. Tavernier, F. Destruhaut, Evaluation of a self-etch primer containing acrylophosphonic acid and HEMA monomers on human dentin, *Oral Health and Care* 4 (2019) 2-7.
- [35] M. Ferrari, F.R. Tay, Technique sensitivity in bonding to vital, acid-etched dentin. *Oper. Dent.* 28 (2003) 3-8.
- 495 [36] P. Duan, K. Schmidt-Rohr, Composite-pulse and partially dipolar dephased multiCP for improved quantitative solid-state ^{13}C NMR, *J. Magn. Res.* 285 (2017) 68-78.
- [37] A. S. Andreev, V. Livadaris, Characterization of catalytic materials through a facile approach to probe OH groups by Solid-State NMR, *J. Phys. Chem. C* 121 (2017) 14108–14119.
- [38] N. Baccile, G. Laurent, C. Bonhomme, P. Innocenzi, F. Babonneau, Solid-State NMR
500 characterization of the surfactant-silica interface in templated silicas: acidic versus basic conditions, *Chem. Mater.* 19 (2007) 1343–1354.
- [39] B. Kumari, M. Brodrecht, T. Gutmann, H. Breitzke, G. Buntkowsky, Efficient Referencing of FSLG CPMAS HETCOR Spectra Using 2D ^1H - ^1H MAS FSLG. *Appl. Magn. Reson.* 50 (2019) 1399–1407.
- 505 [40] B. Hu, J. Trébosc, J.P. Amoureux, Comparison of several hetero-nuclear dipolar recoupling NMR methods to be used in MAS HMQC/HSQC, *J. Magn. Reson.* 192 (2008) 112-122.
- [41] A.L. Boskey, Amorphous calcium phosphate: the contention of bone, *J. Dent. Res.* 76 (1997) 1433–1436.
- [42] C. Combes, C. Rey, Amorphous calcium phosphates: synthesis, properties and uses in
510 biomaterials, *Acta Biomater.* 6 (2010) 3362–3378.
- [43] J. Tropp, N.C. Blumenthal, J.S. Waugh, Phosphorus NMR-study of solid amorphous calcium phosphate, *J. Am. Chem. Soc.* 105 (1983) 22–26.
- [44] S.V. Dorozhkin, Amorphous calcium orthophosphates: nature, chemistry and biomedical applications, *Int. J. Mater. Chem.* 2 (2012) 19–46.

- 515 [45] B. Wopenka, J. Pasteris, A mineralogical perspective on the apatite in bone, *Mater. Sci. Eng. C* 25 (2005) 131–143.
- [46] C. Jäger, T. Welzel, W. Meyer-Zaika, M. Epple, A solid-state NMR investigation of the structure of nanocrystalline hydroxyapatite, *Magn. Reson. Chem.* 44 (2006) 573–580.
- 520 [47] R. Mathew, P.N. Gunawidjaja, I. Izquierdo-Barba, K. Jansson, A. García, D. Arcos, M. Vallet-Regí, M. Edén, Solid-State ^{31}P and ^1H NMR Investigations of amorphous and crystalline calcium phosphates grown biomimetically from a mesoporous bioactive glass, *J. Phys. Chem. C* 115 (2011) 20572–20582.
- [48] J. P. Yesinowski, H. Eckert, Hydrogen environments in calcium phosphates: ^1H MAS NMR at high spinning speeds, *J. Am. Chem. Soc.* 109 (1987) 6274–6282.
- 525 [49] B. Berglund, R. W. Vaughan, Correlations between proton chemical shift tensors, deuterium quadrupole couplings, and bond distances in solids, *J. Chem. Phys.* 73 (1980) 2037–2043.
- [50] E. Brunner, U. Sternberg, Solid-state NMR investigations on the nature of hydrogen bonds, *Prog. Nucl. Magn. Reson. Spectrosc.* 32 (1998) 21–57.
- 530 [51] M. Ben Osman, S. Diallo-Garcia, V. Herledan, D. Brouri, T. Yoshioka, J. Kubo, Y. Millot, G. Costentin, Discrimination of surface and bulk Structure of crystalline hydroxyapatite nanoparticles by NMR. *J. Phys. Chem. C* 119 (2015) 23008–23020.
- [52] A. Kafak-Hachulska, A. Samoson, W. Kolodziejcki, ^1H MAS and $^1\text{H}\rightarrow^{31}\text{P}$ CP/MAS NMR study of human bone mineral, *Calcif. Tissue Int.* 73 (2003) 476–486.
- 535 [53] H.E. Mason, A. Kozlowski, B. L. Phillips, Solid-state NMR study of the role of H and Na in AB-type carbonate hydroxylapatite, *Chem. Mater.* 20 (2008) 294–302.
- [54] T. Azais, S. Von Euw, W. Ajili, S. Auzoux-Bordenave, P. Bertani, D. Gajan, L. Emsley, N. Nassif, A. Lesage, Structural description of surfaces and interfaces in biominerals by DNP SENS, *Solid State Nucl. Magn. Reson.* 102 (2019) 2–11.

